

Numerical investigation of astrophysical cyclotron emission processes

D. C. Speirs¹, S. L. McConville¹, K. M. Gillespie¹, A. D. R. Phelps¹,
A. W. Cross¹, R. A. Cairns², I. Vorgul², R. Bingham^{1,3}, B. J. Kellett³ and K. Ronald¹

¹*SUPA, Department of Physics, University of Strathclyde, Glasgow, G4 0NG, U.K.*

²*School of Mathematics and Statistics, University of St Andrews, St Andrews, KY16 9SS, U.K.*

³*Space Physics Division, STFC, Rutherford Appleton Laboratory, Didcot, OX11 0QX, U.K.*

Astrophysical radio emissions in association with non-uniform magnetic fields have been a subject of interest and debate over the last thirty years [1]. Numerous such sources, including planetary and stellar auroral radio emissions are spectrally well defined with a high degree of extraordinary (X-mode) polarisation. In particular for the terrestrial auroral case, powerful radiation has been observed from field-aligned regions of depleted plasma density ($\omega_{pe} \ll \omega_{ce}$) and it is now widely accepted that such emissions are generated by an electron cyclotron-maser instability driven by a horseshoe shaped electron velocity distribution [2,3]. Such distributions are formed through conservation of magnetic moment when particles descend into the increasing magnetic field of planetary / stellar auroral magnetospheres. In the terrestrial auroral case, the resultant rf emission comprises a spectrum of narrowband components, polarised in the X-mode and centred around ~ 300 kHz. The mean output power of ~ 1 GW corresponds to $\sim 1\%$ of the precipitating auroral electron beam power, in agreement with the predictions of kinetic theory for X-mode dispersion and growth due to an electron horseshoe distribution [2].

A programme of scaled laboratory experiments and simulations (at GHz frequencies) has been undertaken at Strathclyde [3-7], based on the theoretical concept that only the relative magnitudes of the plasma and cyclotron frequencies are fundamental to the dynamics of the instability. Cyclotron resonant energy transfer was observed between an electron horseshoe distribution and transverse electric (TE) modes of an interaction waveguide, with RF conversion efficiencies of the order of 1-2%. In the current context, to improve comparison with the astrophysical case we present results from PiC (Particle-in-cell) code simulations of the dynamics of the cyclotron emission process in the absence of cavity / waveguide boundaries. The 2D axisymmetric version of the finite-difference time domain PiC code KARAT was used, allowing the distribution of particles in the transverse plane of motion to be monitored via the particle population density in plots of v_0 vs v_r . This facilitates the

diagnosis of cyclotron-resonant bunching effects in relative electron orbital phase. For the purpose of simulating the unbounded interaction geometry, a 44cm radius region with radially increasing conductivity was defined around the beam propagation path. This represented an idealised absorber of electromagnetic radiation, inhibiting reflection and the formation of boundary resonant eigenmodes. An electron beam was injected into this simulation geometry with a predefined horseshoe distribution, comprising a pitch spread $\alpha = v_{\perp} / v_z$ of $0 \rightarrow 9.5$, beam energy of $20\text{keV} \pm 5\%$ and beam current of 14A. Other simulation parameters included a uniform axial magnetic flux density of 0.1T, grid resolution of 0.25cm, PiC particle merging factor of 3×10^6 electrons / PiC particle and a total simulation length (beam propagation path) of 4m.

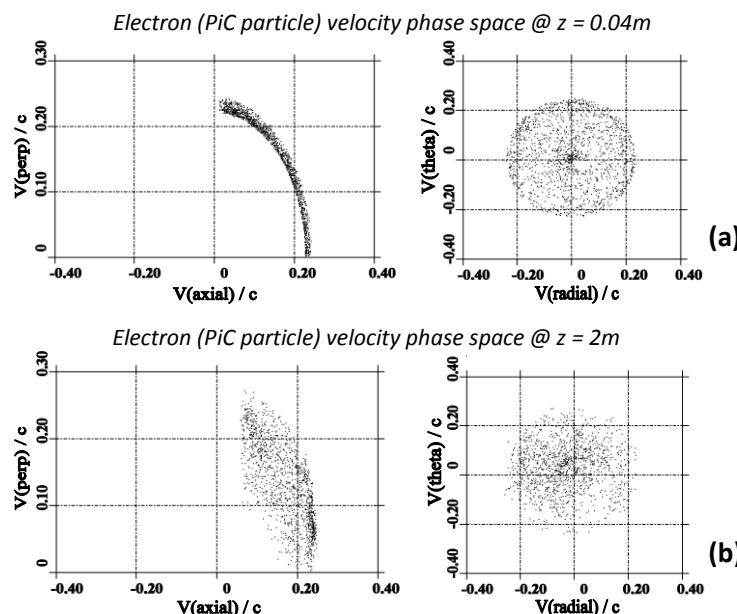


Figure 1. PiC particle velocity distributions measured on transverse planes within the simulation geometry at (a) $z = 0.04\text{m}$ and (b) $z = 2\text{m}$.

Figure 1 shows the PiC particle velocity distributions at two axial positions within the unbounded simulation geometry after a 200ns run. The injected beam distribution at $z = 0.04\text{m}$ contains a well defined pitch spread in v_{\perp} vs v_z and no evidence of cyclotron bunching effects in the associated v_{θ} vs v_r plot. At an axial position of $z = 2\text{m}$ however the picture is very different, with marked smearing in the transverse velocity profile of v_{\perp} vs v_z and evidence of electron bunching / phase-trapping in the corresponding v_{θ} vs v_r plot, characterised by a non uniform concentration of PiC particles extending to the origin. Both effects serve as clear evidence for beam-wave energy transfer and the action of a cyclotron maser instability.

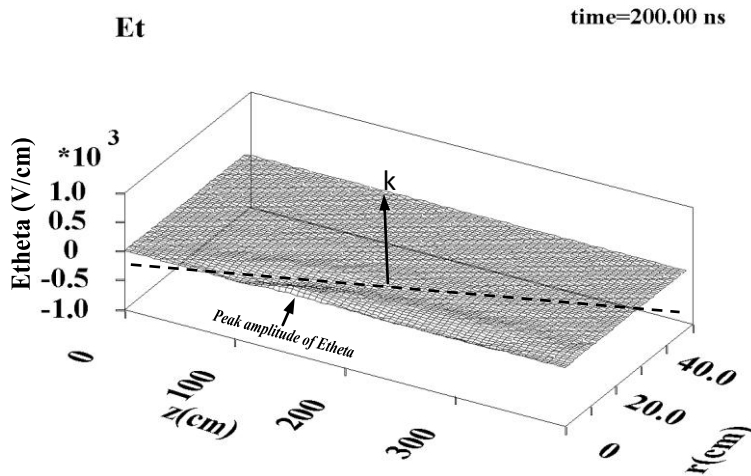


Figure 2. 3D contour plot of E_θ within the unbounded simulation geometry.

Figure 2 contains a 3D contour plot of E_θ over the simulation geometry after a 200ns run. An electromagnetic wave sourced at $z \sim 1.45\text{m}$ is evident propagating near perpendicular to the electron beam with a small backward wave component in the wavevector. A plot of the corresponding radial Poynting flux is presented in figure 3a measured in a plane at $r = 3.5\text{cm}$, over the 4m length of the simulation geometry. A DC offset is present in the measurement due to low frequency EM field components associated with the electron beam propagation. After 180ns a peak rf output power of $\sim 3\text{kW}$ was measured corresponding to an rf conversion efficiency of 1.1%. This is comparable to the $\sim 1\%$ efficiency obtained from waveguide bounded simulations [3,6] and consistent with the estimate of $\sim 1\%$ for the astrophysical phenomena [8,9]. The corresponding output spectrum is presented in figure 3b, showing a well defined signal at 2.68GHz. This represents a 1.1% downshift from the relativistic electron cyclotron frequency of 2.71GHz, consistent with the slight backward wave character observed in figure 2.

In conclusion, PiC simulations have been conducted to investigate the dynamics of the cyclotron emission process attributed to numerous astrophysical radio sources [1,8,9] in the absence of cavity boundaries. Computations reveal that a well-defined cyclotron emission process occurs, albeit with a low spatial growth rate compared to waveguide bounded cases [3,6]. RF output is near perpendicular to the electron beam with a slight backward-wave character and well defined spectral output centred just below the relativistic electron cyclotron frequency. The corresponding RF conversion efficiency of 1.1% is comparable to waveguide bounded simulations [3,6] and consistent with the predictions of theory [2] and estimates of

~1% for the astrophysical phenomena [8,9].

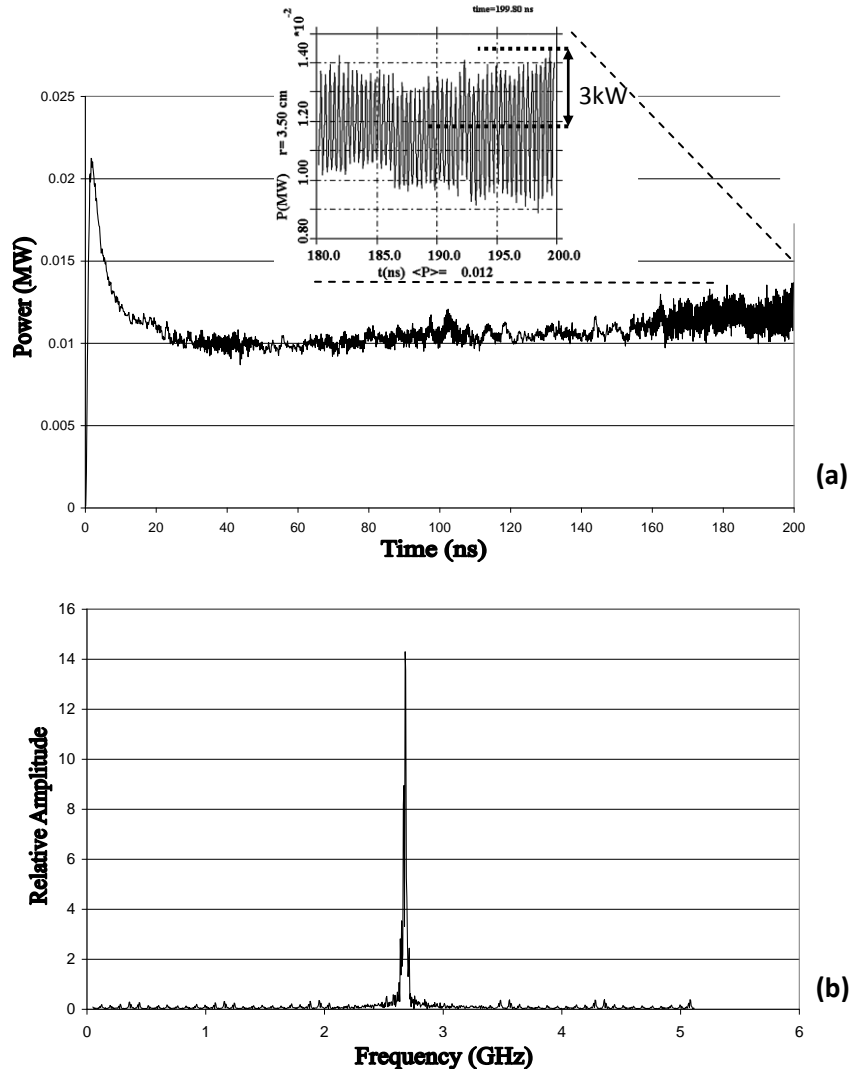


Figure 3: (a) Temporal evolution of the radial Poynting flux measured in a plane at $r = 3.5\text{cm}$ spanning the length of the simulation. (b) Fourier transform of E_0 from $t = 0 \rightarrow 200\text{ns}$ at $z = 1.9\text{m}$.

Acknowledgements

The EPSRC and the STFC Centre for Fundamental Physics supported this work. Prof V.L. Tarakanov is thanked for his assistance with the numerical models.

References

- [1] A.P. Zarka, *Advances in Space Research*, **12**, 99 (1992).
- [2] R. Bingham and R. A. Cairns, *Phys. Plasmas*, **7**, 3089 (2000).
- [3] K.M. Gillespie, D.C. Speirs, K. Ronald et al., *Plasma Phys. Control. Fusion*, **50**, 124038 (2008).
- [4] S.L. McConville, D.C. Speirs, K. Ronald et al., *Plasma Phys. Controlled Fusion*, **50**, 074010 (2008).
- [5] K. Ronald, D.C. Speirs, S.L. McConville et al., *Phys. Plasmas*, **15**, 056503 (2008).
- [6] D.C. Speirs, K. Ronald, S.L. McConville et al., *Phys. Plasma*, **17**, 056501 (2010).
- [7] K. Ronald, D.C. Speirs, S.L. McConville et al., *Plasma Phys. Control. Fusion*, **53**, 074015 (2011).
- [8] P.L. Pritchett and R.J. Strangeway, *J. Geophys. Res.*, **90**, 9650 (1985).
- [9] D.A. Gurnett, *J. Geophys. Res.*, **79**, 4227 (1974).